

## **Structural Origins of High-Affinity Biotin Binding to Streptavidin**

PATRICIA C. WEBER, D. H. OHLENDORF, J. J. WENDOLOSKI,  
AND F. R. SALEMME\*

# Structural Origins of High-Affinity Biotin Binding to Streptavidin

PATRICIA C. WEBER, D. H. OHLENDORF, J. J. WENDOLOSKI,  
F. R. SALEMME\*

The high affinity of the noncovalent interaction between biotin and streptavidin forms the basis for many diagnostic assays that require the formation of an irreversible and specific linkage between biological macromolecules. Comparison of the refined crystal structures of apo and a streptavidin:biotin complex shows that the high affinity results from several factors. These factors include the formation of multiple hydrogen bonds and van der Waals interactions between biotin and the protein, together with the ordering of surface polypeptide loops that bury the biotin in the protein interior. Structural alterations at the biotin binding site produce quaternary changes in the streptavidin tetramer. These changes apparently propagate through cooperative deformations in the twisted  $\beta$  sheets that link tetramer subunits.

**S**TREPTAVIDIN IS A TETRAMERIC PROTEIN (molecular weight =  $4 \times 15,000$ ) isolated from the actinobacterium *Streptomyces avidinii* (1). Streptavidin, and the homologous protein avidin, are remarkable for their ability to bind up to four molecules of *D*-biotin with unusually high affinity [dissociation constant  $K_d = 10^{-15}M$  (1, 2)]. Although these proteins may function as antibiotics that deplete the environment of the essential vitamin biotin, they have been studied primarily as paradigms for understanding high-affinity protein-ligand interactions (2). At the same time, the ability of streptavidin and avidin to bind derivatized forms of biotin has led to their widespread use in diagnostic assays that require formation of an essentially irreversible and specific linkage between biological macromolecules (3). We undertook the structure determination of streptavidin, with and without bound biotin, to uncover the origins of high affinity of the protein for biotin.

Streptavidin was obtained from several commercial sources and produced different crystal forms during the course of the study. The most consistent results were obtained with a fragment of the native 159-residue streptavidin chain, incorporating residues 13 through 133. Numerous studies indicate that this truncated form of the molecule

binds biotin with an affinity that is the same or similar to alternative longer versions of the protein. Moreover, in some cases it appeared that preparations identified as full-length material crystallized isomorphously with the truncated fragment, suggesting that the molecular termini may be relatively flexible or disordered. Crystallization conditions for apostreptavidin and its biotin complex were found by robotic grid search methods (4). Both formed crystals from a polyethylene glycol-LiCl mixture, although the streptavidin:biotin complex crystallizes at pH 7.8 [space group  $I4_122$ ,  $a = b = 99.4$  Å,  $c = 125.8$  Å (5)], whereas apostreptavidin crystallizes at pH 2.4 [space group  $I4_122$ ,  $a = b = 58.3$  Å,  $c = 172.5$  Å]. Unit cell parameters of truncated apostreptavidin are similar to those reported by Pahler *et al.* (6), although the crystals studied here grow at lower pH, and diffract to higher resolution ( $d_{\min} = 1.7$  Å).

The structure of apostreptavidin was determined by multiple isomorphous replacement techniques. X-ray diffraction data for parent crystals and several isomorphous replacement derivatives were collected using a multiwire area detector and processed with the Xengen data-reduction package (7). Successful derivatives included  $K_2Pt(SCN)_6$ , which was prepared by soaking crystals in the heavy metal solution, and an iodine derivative prepared by crystallizing protein after reaction in solution (8). Substitution sites were located by an automated search procedure (9) performed on the heavy atom difference Patterson maps. Phases were ob-

Central Research & Development Department, E. I. du Pont de Nemours and Company, Inc., Du Pont Experimental Station, ES 228/320, Wilmington, DE 19880-0228.

\*To whom correspondence should be addressed.

tained after refinement of heavy atom positions by the origin-removed different Patterson method (10) and used to compute a 2.6 Å resolution electron density map (11).

The electron density map was interpreted with the graphics program FRODO (12). Identification of several Trp and other large residues allowed an initial  $\alpha$ -carbon backbone trace and sequence assignment to be made for ~70% of the structure, organized primarily as antiparallel  $\beta$  sheet. A partial atomic model was constructed from the  $\alpha$ -carbon trace with the use of fragment superposition (13) from a database of refined protein structures (14). Complete backbone fragments that best fit the  $\alpha$ -carbon trace were incorporated into the model. Side chains were positioned by displaying possible rotamers for each amino acid from a library (15) and by including coordinates for the rotamer that best fit the electron density. Phases computed from the partial model were combined with the multiple isomorphous replacement phases and used to generate an improved electron density map whose interpretation defined the remainder of the molecular structure. The structure was refined with the restrained least-squares method of Hendrickson and Konnert (16) and manual rebuildings in electron density maps. Although the refinement proceeded smoothly, two surface loops lacked defined density and appeared disordered in the final structure. The crystallographic *R*-factor for apostreptavidin, including residues 13 to 46, 49 to 63, and 69 to 133, as well as 33 water molecules, is 0.21 for 11,120 reflections [ $F_{\text{observed}} > \sigma(F_{\text{observed}})$ ] between 5.0 and 1.8 Å resolution.

The structure of the streptavidin:biotin complex was solved with the use of symmetry-constrained searches of the complex unit cell with the apostreptavidin tetramer (17). Apostreptavidin crystallizes with a monomer in the asymmetric unit, so that subunits of the tetramer are related by crystallographic dyad axes. Since tetramers in the nonisomorphous crystals of the streptavidin:biotin complex could also pack with subunits related by crystal symmetry, we searched that cell using the apostreptavidin tetramer as the probe molecule (18). A maximum correlation coefficient of 0.56 was obtained for 1363 intensities between 4 and 5 Å resolution when the streptavidin tetramer was positioned at the origin of the streptavidin:biotin complex unit cell with all three of its dyad axes coincident with the crystallographic dyad axes. This result shows that both apo and liganded forms of streptavidin are tetramers with subunits related by 222 point group symmetry. The initial crystallographic *R*-factor for apostreptavidin positioned in the biotin:streptavidin unit cell

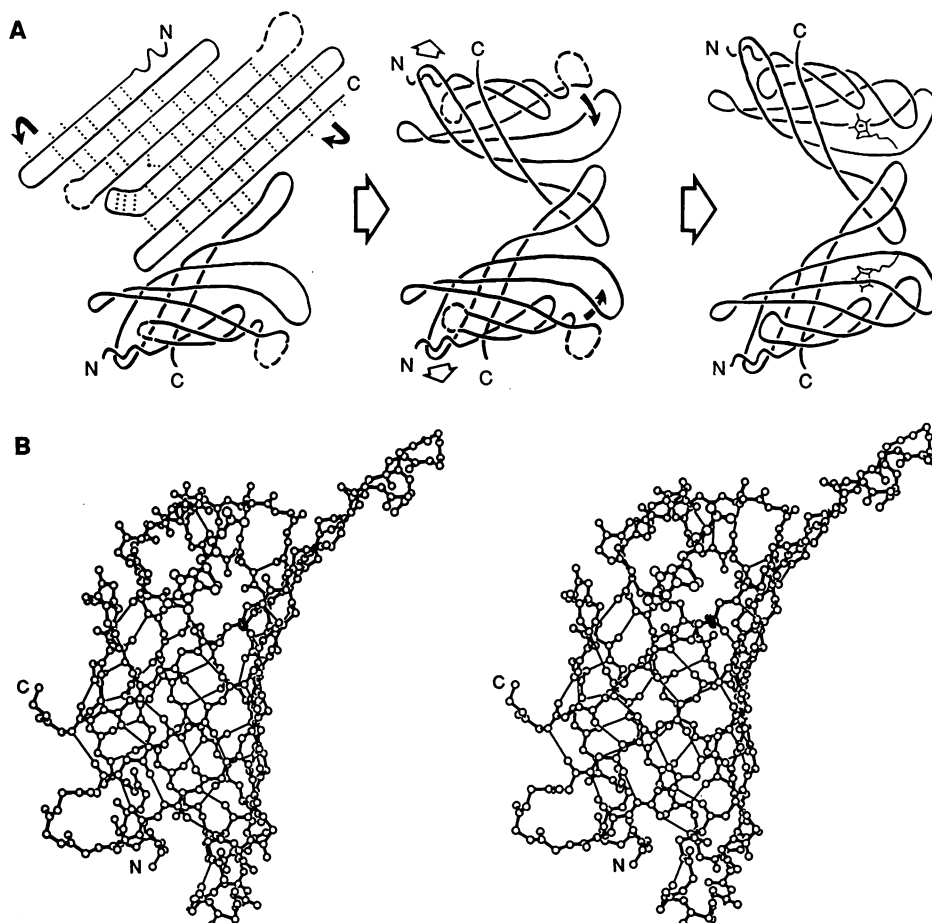


**Fig. 1.** Streptavidin structure. (A) Cartoon sequentially showing the  $\beta$  sheet folding pan of the hydrogen-bonded dimer, the apostreptavidin structure, and changes upon biotin binding. These changes include ordering of two loops (shown dashed) incorporating residues 45 to 50 and 63 to 69. (B) Stereoview of a streptavidin subunit with biotin bound, showing  $\beta$  barrel hydrogen bonds as thin lines. Residues 13 through 133 form an eight-stranded antiparallel  $\beta$  sheet wrapped as a slightly flattened barrel.

was 0.41 for data from 5.0 to 2.6 Å resolution.

The structure of the streptavidin:biotin complex was refined by a combination of conventional restrained least-squares methods and crystallographically constrained molecular dynamics. The molecular dynamics refinement protocol essentially followed previous work (19), but was implemented in our laboratory by combining features of AMBER (20), PROLSQ (16), and PROFFT (21). The crystallographic *R*-factor of the streptavidin:biotin complex, including all residues between sequence positions 13 and 133, biotin, and nine water molecules, is 0.22 for 7379 reflections with  $F_{\text{observed}} > \sigma(F_{\text{observed}})$  between 5.0 and 2.6 Å resolution [coordinates will be deposited in the Brookhaven Protein Data Bank (14)].

Streptavidin subunits are organized as eight-stranded, sequentially connected, antiparallel  $\beta$  sheets. The sheets are formed of coiled polypeptide chains with a staggered pattern of adjacent strand hydrogen-bond registration (22). This arrangement pro-

duces a cyclically hydrogen-bonded barrel with several extended hairpin loops, including one near the carboxyl terminus whose edge is free to form a more extended  $\beta$  sheet (Fig. 1). Pairs of streptavidin barrels hydrogen bond together at this free edge to form symmetric dimers that resemble basketball nets connected by their rims at a 45° angle. The naturally occurring streptavidin tetramer is formed by interdigitating a pair of dimers, with their dyad axes coincident, to produce a particle with 222 point group symmetry. The tetramer is stabilized by extensive van der Waals interactions between the subunit barrel surfaces, which have complementary curvatures (Fig. 2).

Biotin binds in pockets at the ends of each of the streptavidin  $\beta$  barrels (Fig. 1). The residues lining the pockets are primarily aromatic or polar amino acids or both. These groups are solvent exposed in apostreptavidin so that several water molecules occupy the biotin binding site. Biotin binding involves displacement of bound water, formation of multiple interactions between biotin heteroatoms and the binding site

residues, and burial of the biotin through ordering of a surface loop (residues 45 to 50) that is disordered in apotreptavidin. Polar interactions made between biotin heteroat-

oms and the protein include (i) an extensive pattern of hydrogen bonds with the biotin ureido group, where no less than five protein residues form associations; (ii) a possi-

ble interaction between biotin sulfur and the hydroxyl group of Thr<sup>90</sup>; and (iii) hydrogen-bonded interactions with the valeryl carboxyl group that includes a hydrogen bond from the backbone NH of Asn<sup>49</sup>, which becomes ordered on biotin binding (Fig. 3). Several other residues lining the binding site are immobilized by hydrogen bonds, which are formed in many cases with the same residues that hydrogen bond to biotin. These include Trp residues 79, 92, and 108 that pack around the biotin tetrahydrothiophene ring, and which, together with Trp<sup>120</sup> from the cyad-related subunit, form a hydrophobic biotin binding site. As a result of this extensive pattern of interactions, resulting in part from the ordering of loop 45 to 50, bound biotin is essentially buried in the complex with only the valeryl carboxyl oxygens partially accessible to solvent.

Experimental studies of the binding of biotin analogs to avidin, a tetrameric protein from avian egg white that shares 38% sequence identity (23) with the crystallographically defined streptavidin, suggest that interactions made with the ureido ring system predominate in stabilizing the biotin-protein complex (2). An unusual aspect of the interaction involves participation of the bio-

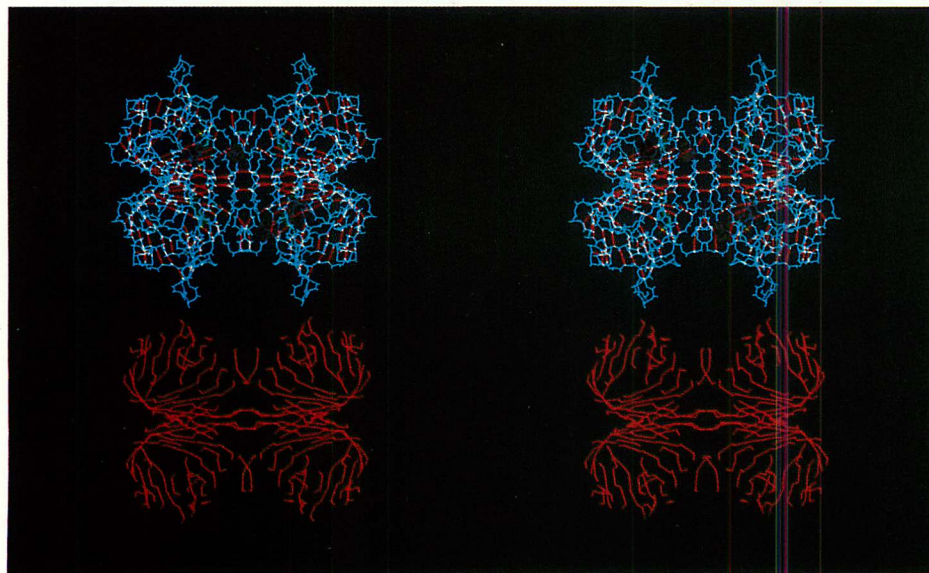


**Fig. 2.** Stereoviews of the streptavidin tetramer. (**Top**) Tetramer with bound biotins (backbone atoms), viewed along dyad symmetry axis relating hydrogen-bonded subunits (hydrogen bonds in red). (**Bottom**) Hydrogen-bond circuit representation of the tetramer, as defined by sheet hydrogen bonds and backbone amide group atoms. This representation emphasizes the continuity of the interactions that distribute forces throughout the barrels and across the subunit dimer axes.

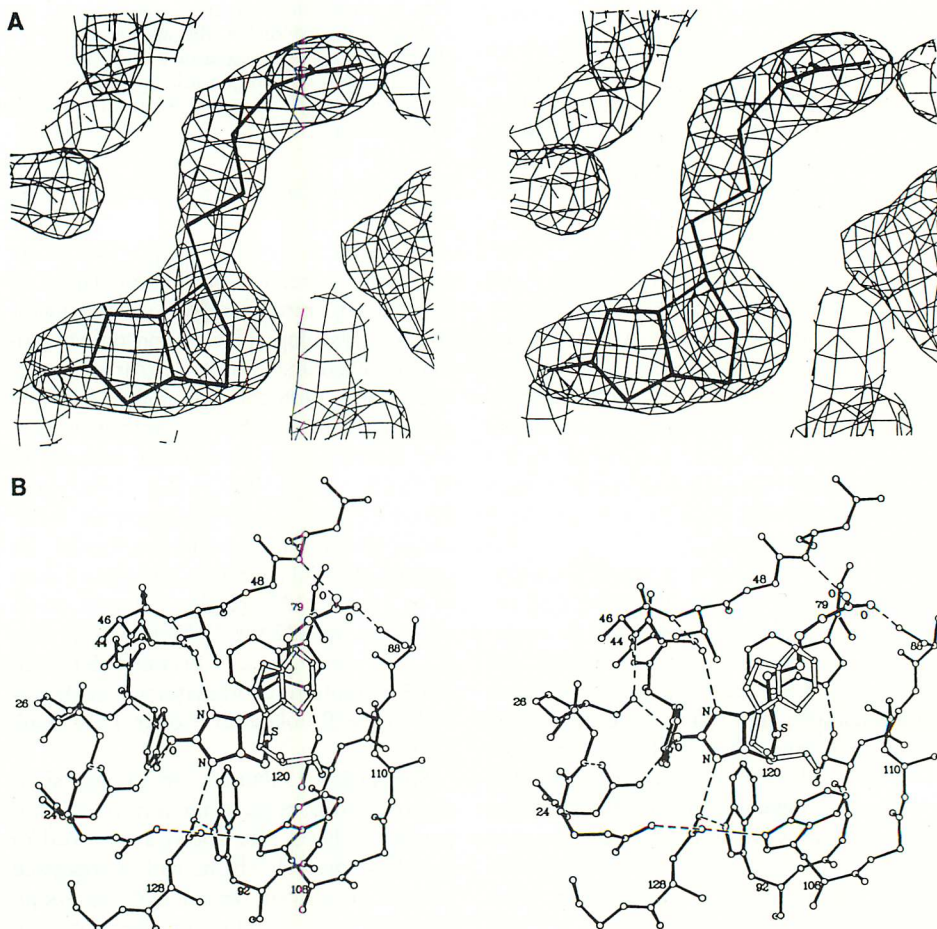


**Fig. 3.** Biotin binding site. (**A**) Biotin electron density from final  $(2F_o - F_c)\alpha_{\text{calc}}$  2.6 Å electron density map. (**B**) Biotin interactions. One indole ring (open bonds) is contributed by Trp<sup>120</sup> from the symmetry-related, hydrogen-bonded dimer. Residues shown include: Asn<sup>23</sup>, Gln, Leu, Gly, Ser<sup>27</sup>, Tyr<sup>43</sup>, Glu, Ser, Ala, Val, Gly, Asn<sup>49</sup>, Trp<sup>79</sup>, Ser<sup>88</sup>, Ala, Thr, Thr, Trp<sup>92</sup>, Trp<sup>108</sup>, Leu, Leu<sup>110</sup>, Asp<sup>128</sup>, and Thr<sup>129</sup>. Some side chains are omitted for clarity. Dashed lines show the hydrogen-bonding pattern for residues that interact with biotin heteroatoms. The valeryl oxygens of biotin are hydrogen-bonded to the backbone NH of Asn<sup>49</sup> and Oγ1 of Ser<sup>88</sup>, respectively. The Thr<sup>90</sup> side chain oxygen is near the biotin sulfur and Trp<sup>79</sup> Ne1. Ser<sup>43</sup> Oγ1 interacts with one biotin ureido NH (upper) and the backbone NH of Val<sup>47</sup>. The other biotin ureido NH (lower) is hydrogen-bonded to a carboxyl oxygen of Asp<sup>128</sup>. The Asp<sup>128</sup> side chain oxygens form additional interactions with Trp<sup>92</sup> Ne1, Trp<sup>108</sup> Ne1, and Gln<sup>24</sup> Ne1. Three side chain atoms, Tyr<sup>43</sup> OH, Asn<sup>23</sup> NδH, and Ser<sup>27</sup> OH, are situated to hydrogen bond with the biotin ureido oxygen. The OH of Ser<sup>27</sup> is also hydrogen-bonded to Ala<sup>46</sup> NH, and Asn<sup>23</sup> Oδ1 interacts with Leu<sup>25</sup> NH. Note that residues forming hydrogen bonds with biotin ureido oxygen are themselves stabilized by orienting hydrogen bonds to backbone NH groups.

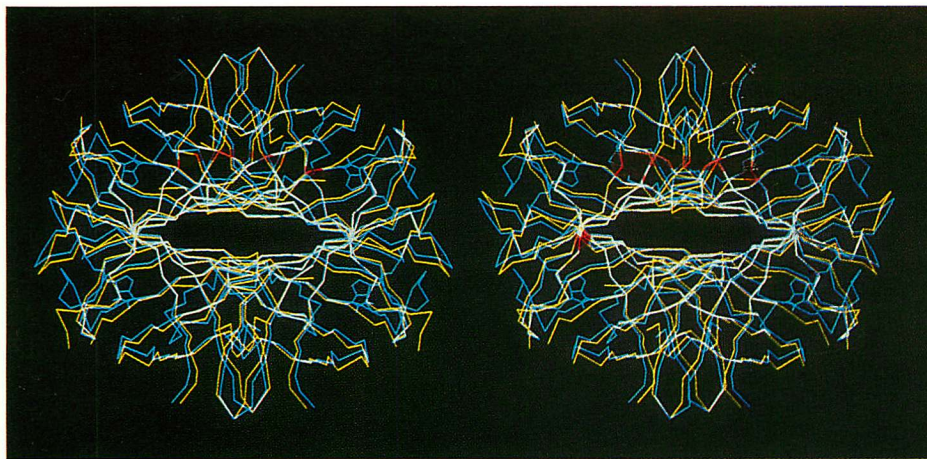


**Fig. 4.** Streptavidin quaternary structural changes. Yellow lines show  $\alpha$ -carbon backbone trace of apostreptavidin and blue lines show streptavidin with biotin bound. Pairs of hydrogen-bonded dimers have been separated by 15 Å along the horizontal tetramer dyad axis for clarity. Changes in the hydrogen-bonded dimer geometry produce relative rotations of the dimers about the horizontal dyad. Tetramer subunits of both the apostreptavidin and streptavidin:biotin complex crystals are related by crystal-symmetry operations. The root-mean-square (rms) displacement for 112 common subunit C $\alpha$  atoms, relative to the origin defined by the intersection of the tetramer 222 symmetry axes is 2.0 Å; the rms fit for the 67 C $\alpha$  atoms in the  $\beta$  barrel is 0.7 Å in this frame. Superpositioning individual subunits gives an rms of 1.9 Å for all 112 C $\alpha$  atoms common to the apo and liganded proteins and 0.3 Å for the 67  $\beta$  barrel C $\alpha$  atoms.

tin ureido group in an extended hydrogen-bond network anchored by the buried carboxyl group of Asp<sup>128</sup> that hydrogen bonds one ureido NH. The latter hydrogen bond could stabilize resonance forms that localize positive charge on biotin nitrogens and negative charge at the biotin ureido oxygen. Indeed, the ureido oxygen forms three hydrogen bonds, arranged with tetrahedral geometry, suggesting that the groups involved stabilize an  $sp^3$  oxyanion (Fig. 3B). Comparison of streptavidin and avian avidin show that all of the groups that directly bind biotin are conserved with the exception of Ser<sup>45</sup>, which is replaced by Thr with similar functionality, and Asp<sup>128</sup>, which, surprisingly, is substituted by Asn (23). These changes may reflect some differences in the way biotin is stabilized in streptavidin and avidin. However, the analog of the residue that hydrogen bonds to Asp<sup>128</sup> in streptavidin, Gln<sup>24</sup>, is substituted by Asp in avidin, so that slightly different but similar polarization networks could be functional in both proteins. Although biotin makes additional hydrophobic and hydrogen-binding interactions that assist binding, the hydrogen-bonded interactions with the valeryl group appear to play a lesser role. This group is partially accessible in the complex and provides the covalent attachment sites for linking biotin with other biomolecules (3).

Apo and liganded streptavidin differ in quaternary structure. Although the observed changes could in part reflect differences in crystal pH or lattice interactions and there is currently no evidence for subunit cooperativity, the pattern of quaternary changes

nevertheless suggests a consistent mechanism of subunit communication. Subunit differences between apo and liganded streptavidin include the formation of extensive biotin:protein interactions, concomitant ordering of two surface loops, and formation of a salt link between Glu<sup>51</sup> and Arg<sup>84</sup> from adjacent loops. Collectively, these interactions cause the subunit barrels to flatten slightly and become more tightly wrapped. Because the subunit barrels are part of a more extended  $\beta$  sheet that forms the hydrogen-bonded dimer (Figs. 1 and 2), and the barrel exteriors pack at the dimer-dimer interface (Figs. 2 and 4), changes in barrel curvature effect both hydrogen-bonded dimer geometry and dimer-dimer packing. The net result of the change in subunit barrel curvature is to alter the twist of  $\beta$  sheet that connects dimer subunits, which produces a slight increase in the angle between the barrel domains. The tetramer adjusts to the changes in dimer sheet twist and preserves the complementary sheet packing by a 5.4° rotation of the dimer subunits around the corresponding tetramer dyad axis (Fig. 4).

The unusually high affinity of streptavidin for biotin reflects participation of a number of factors, the analogs of which have been previously encountered individually in other protein-ligand interactions. These factors include oriented dipole arrays to stabilize bound oxyanions [for example, the oxyanion hole in serine proteases (24)], hydrogen-bond dipole networks to alter charge distribution on bound ligands [such as the serine protease charge relay system (24)], and dis-

order-order transitions to sequester bound ligands from the solvent environment [as in triose phosphate isomerase (25)]. In streptavidin, these factors, together with quaternary changes in structure, combine to produce both strong binding and a high activation energy for dissociation that characterize the near irreversibility of the biotin:streptavidin interaction.

#### REFERENCES AND NOTES

1. L. Chalet and F. J. Wolf, *Arch. Biochem. Biophys.* **106**, 1 (1964).
2. N. M. Green, *Adv. Protein Chem.* **29**, 85 (1975).
3. P. R. Langer, A. A. Waldrop, D. C. Ward, *Proc. Natl. Acad. Sci. U.S.A.* **78**, 6633 (1981); J. J. Leary, D. J. Brigati, D. C. Ward, *ibid.* **80**, 4045 (1983).
4. M. J. Cox and P. C. Weber, *J. Appl. Cryst.* **20**, 366 (1987); *J. Cryst. Growth* **90**, 318 (1988).
5. P. C. Weber, M. J. Cox, F. R. Salemme, D. H. Ohlendorf, *J. Biol. Chem.* **262**, 12728 (1987).
6. A. Pahlert *et al.*, *ibid.*, p. 13933.
7. A. J. Howard *et al.*, *J. Appl. Cryst.* **20**, 383 (1987).
8. J. Wolff and I. Covelli, *Eur. J. Biochem.* **9**, 371 (1969).
9. T. C. Terwilliger *et al.*, *Acta Cryst.* **A43**, 1 (1987).
10. T. C. Terwilliger and D. Eisenberg, *ibid.* **A39**, 813 (1983).
11. The agreement between multiple observed diffraction intensities,  $R_m = \{ \text{rms} [(I_j - \langle I \rangle) / \sigma_j] \}$  (rms, root-mean-square), for 84,062 observations of 9,225 unique reflections to 2.6 Å resolution was 0.054 for the streptavidin:biotin complex, and the  $R_m$  for apostreptavidin native crystals was 0.052 for 89,393 observations of 13,496 observations to 1.7 Å resolution. The fractional difference in diffraction amplitudes to 2.2 Å resolution between native and derivative crystals of apostreptavidin was 0.14 for iodinated apostreptavidin and 0.19 for the crystal soaked in  $K_2Pt(SCN)_6$ . In the apostreptavidin structure determination by multiple isomorphous replacement techniques (10), the mean figure of merit for 4640 reflections to 2.6 Å resolution was 0.62, and the ratio of the mean heavy atom scattering factor to the mean lack of closure ( $f_H/E$ ) was 1.4 for acentric reflections of the platinum derivative and 0.8 for those of the iodinated apostreptavidin.
12. T. A. Jones, *J. Appl. Cryst.* **11**, 268 (1978).
13. — and S. Thirup, *EMBO J.* **5**, 819 (1986); B. C. Finzel, *Protein Struct. Funct. Genet.*, in press.
14. F. C. Bernstein *et al.*, *J. Mol. Biol.* **112**, 535 (1977).
15. J. W. Ponder and F. M. Richards, *ibid.* **193**, 775 (1987).
16. W. A. Hendrickson and J. H. Koonert, in *Biomolecular Structure, Function, Conformation and Evolution*, R. Srinivasan, Ed. (Pergamon, Oxford, 1980), vol. 1, pp. 43–57.
17. M. Fujinaga and R. Read, *J. Appl. Cryst.* **20**, 517 (1987).
18. The apostreptavidin tetramer was positioned with a twofold symmetry axis coincident with a crystallographic dyad axis of the streptavidin:biotin unit cell. The correlation coefficient between observed and calculated structure factors was calculated for each orientation of the tetramer as it was rotated 180° in 3° steps about, and translated in 1 Å increments along, the crystal twofold axes.
19. A. T. Brünger, *J. Mol. Biol.* **203**, 803 (1988).
20. P. Weiner and P. A. Kollman, *J. Comput. Chem.* **2**, 287 (1981); S. J. Weiner *et al.*, *J. Am. Chem. Soc.* **106**, 765 (1984).
21. B. C. Finzel, *J. Appl. Cryst.* **20**, 53 (1987).
22. F. R. Salemme, *Prog. Biophys. Mol. Biol.* **42**, 95 (1983).
23. C. E. Argarona, I. D. Kuntz, S. Birken, R. Axel, C. R. Cantor, *Nucleic Acids Res.* **14**, 1871 (1986).
24. J. Kraut, *Annu. Rev. Biochem.* **46**, 331 (1977).
25. T. C. Alber *et al.*, *Cold Spring Harbor Symp. Quant. Biol.* **52**, 603 (1987).
26. The structure of a streptavidin:biotin complex has been determined independently by W. A. Hendrickson *et al.* (*Proc. Natl. Acad. Sci. U.S.A.*, in press).

4 November 1988; accepted 12 December 1988